

GRADUATE SCHOOL OF NEURAL AND  
BEHAVIORAL SCIENCES

FACULTY OF SCIENCE  
FACULTY OF MEDICINE

EBERHARD-KARLS-UNIVERSITÄT TÜBINGEN

CHARITÉ BERLIN

# Evolution of Beta Bursts in the 6-OHDA Rat Model

Thesis

submitted in partial fulfilment of the degree  
requirements

**Master of Science**

*Presented by*  
Franziska PELLEGRINI

*Supervisors:*  
Dr. Wolf-Julian NEUMANN, Prof. Andrea KÜHN  
Berlin, September 5, 2018

Thesis Advisor:

Prof. Dr. Andrea Kühn

Movement disorders and neuromodulation section, Charité Berlin

Second Reader:

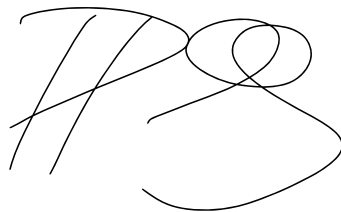
Dr. Markus Siegel

Large scale neural interactions group, Centre for Integrative Neuroscience  
Tübingen

- I affirm that I have written the dissertation myself and have not used any sources and aids other than those indicated.
- I affirm that I have not included data generated in one of my laboratory rotations and already presented in the respective laboratory report

Date/ Signature:

5.9.2018

A handwritten signature in black ink, consisting of a stylized 'M' followed by a large, looping 'S'.

## **Abstract**

Cortical and subcortical beta activity is closely related to dopaminergic degeneration and motor symptoms in Parkinson's Disease. Here we study the relationship of electrophysiological data, recorded in the subthalamic nucleus (STN) and primary motor cortex (M1), behavioral ability and neuron degeneration. More specifically, we investigate different beta burst parameters in the 6-hydroxydopamine (6-OHDA) rat model. We show that burst parameters are correlated with histological changes. Moreover, beta power and the proportion of long bursts provide the best predictions on the actual dopaminergic stage. Employing linear discriminant analysis, we distinguish healthy from lesioned animals with an accuracy of over 80 %.

## Acknowledgements

I would like to thank Dr. Wolf-Julian Neumann and Prof. Andrea Kühn for supervision, Dr. Christoph van Riesen and Dr. Jens Haumesser for providing me with the data and good advice, and Dr. Roxanne Lofredi and Dr. Andreas Horn for valuable comments and critique regarding the project.

# Contents

<b>1</b>	<b>Introduction</b>	<b>1</b>
<b>2</b>	<b>Material and Methods</b>	<b>3</b>
2.1	Experiment . . . . .	3
2.2	Data Analysis . . . . .	6
<b>3</b>	<b>Results</b>	<b>9</b>
3.1	Behavior . . . . .	9
3.2	Histology . . . . .	10
3.3	Beta Power . . . . .	10
3.4	Burst Duration . . . . .	12
3.5	Time spent in bursts . . . . .	12
3.6	Burst Amplitude . . . . .	15
3.7	Overlapping Bursts . . . . .	15
3.8	Correlation between Burst Duration and Amplitude . . . . .	15
3.9	Correlation without Control Group . . . . .	16
3.10	Partial Correlations . . . . .	16
3.11	Low and High Beta . . . . .	16
3.12	Stepwise Regression . . . . .	16
3.13	Classification . . . . .	17
<b>4</b>	<b>Discussion</b>	<b>19</b>
<b>5</b>	<b>Conclusion</b>	<b>24</b>
	<b>Supplementary Material</b>	<b>25</b>

## List of Figures

1	Experimental design. . . . .	4
2	Definition of bursts. . . . .	8
3	Average test data per group. . . . .	11
4	Burst durations per group. . . . .	13
5	Original and estimated histology scores. . . . .	18
S1	Power–histology correlation. . . . .	26
S2	Correlation between proportional number of long bursts and histology. . . . .	26
S3	Correlation between time spent in bursts and histology. . . . .	27
S4	Amplitude–histology correlation. . . . .	27
S5	Correlation between the burst overlap and histology. . . . .	28
S6	Correlation between burst duration and burst amplitude. . . . .	28
S7	Original and predicted histology scores without subjects. . . . .	29
S8	Original and estimated histology scores without subjects of zero long bursts. . . . .	30
S9	Original and predicted histology scores without subjects with- out subjects with zero long bursts. . . . .	31

## List of Tables

1	Spearman's rank correlations between electrophysiological parameters and histology. . . . .	14
S1	Group averages and standard error of the mean for all parameters. . . . .	25

## Abbreviations

**6-OHDA** 6-hydroxydopamine

**a.u.** arbitrary units

**DBS** Deep brain stimulation

**LDA** Linear discriminant analysis

**LFP** Local field potential

**M1** Primary motor cortex

**PD** Parkinson's disease

**SD** Standard deviation

**SNc** Substantia nigra pars compacta

**STN** Subthalamic nucleus

**STR** Striatum

**TFR** Time–frequency representation

**TH** Tyrosine hydroxylase

**UPDRS** Unified Parkinson's disease rating scale

**w/o c** without control group



# 1 Introduction

With an overall prevalence of 571 per 100 000 (across different countries), Parkinson’s disease (PD) is one of the most common neurological disorders (Pringsheim et al., 2014). Prevalence appears to increase with age (Pringsheim et al., 2014). According to the *International Parkinson and Movement Disorder Society Clinical Diagnostic Criteria for Parkinson’s disease* (Postuma et al., 2015), the diagnosis of PD is based on three cardinal motor symptoms: bradykinesia (slowness of movements) in combination with either rest tremor (trembling of a fully resting limb), rigidity (muscle stiffness) or both. Further possible symptoms include cognitive impairments, depression, sleep disorders, functional anosmia and autonomic dysfunctions (Schapira et al., 2015).

PD is characterized by a progressive cell loss of the pars compacta of the substantia nigra, leading to deficient nigral dopaminergic output and degeneration of striatal fibers (Bergman et al., 1990). Apparently, an overactivity in several nuclei of the basal ganglia plays a major role in development of motor abnormalities. Lesioning the STN in parkinsonian monkeys leads to reduction of motor impairments (Bergman et al., 1990). In the past years this finding was used to develop deep brain stimulation (DBS) as a therapy for PD patients (Little et al., 2013). Here, the STN is stimulated with very high frequencies, leading to a great reduction of motor symptoms (Schuepbach et al., 2013; Deuschl et al., 2006). Also the Striatum (STR) is part of the network. It receives the main input from cortex and thalamus (Haber, 2003) and outputs to some of the basal ganglia nuclei and indirectly also to the STN (Nambu et al., 1998).

Symptom severity of PD is closely related to beta oscillations (around 13 to 30 Hz) in the basal ganglia (Kühn et al., 2006): for example, Neumann and colleagues (Neumann et al., 2016) found that exaggerated beta band power, measured in the STN of PD patients in the hypodopaminergic state, was associated with higher scores on the *Unified Parkinson’s Disease Rating Scale* (UPDRS-III).

Pathological beta oscillations have been studied both in human patients (Kühn et al., 2006; Tinkhauser et al., 2017a; Tinkhauser et al., 2017b) and in animal models (Beck et al., 2016; Feingold et al., 2015). The 6-hydroxydopamine (6-OHDA) rat model of PD mimics the human disease closely (Deumens et al., 2002) as it also leads to a degeneration of dopaminergic neurons in the substantia nigra. Several studies found exaggerated beta

band activity in 6-OHDA lesioned rats (Sharott et al., 2005; Beck et al., 2016). In comparison to other models, like the reserpine model, the 6-OHDA lesion proceeds chronic-progressively. Thus, the 6-OHDA lesion gets more severe with time after the injection. This model property poses a unique opportunity to observe the evolution of behavioral, electrophysiological, and physiological symptoms over time and progressing degeneration. After approximately 20 days, the degeneration of the dopaminergic nigrostriatal system is complete and remains stable afterwards (Beck et al., 2016).

Studying oscillations in the basal ganglia in more detail, several studies found that beta activity occurs in brief events lasting less than 150 ms (Feingold et al., 2015; Shin et al., 2017; Tinkhauser et al., 2017a). While short-lived bursts appear to play a functional role in the basal ganglia–cortical motor circuit (Feingold et al., 2015), bursts of longer duration relate to pathological motor impairments like stiffness and slowness in PD (Tinkhauser et al., 2017a; Tinkhauser et al., 2017b). The duration of beta bursts is positively correlated with the burst amplitude (Tinkhauser et al., 2017a).

The specific relation between beta burst characteristics and nigral cell loss has not been investigated so far. The study at hand aims at forging a bridge among PD motor symptoms, beta burst characteristics, and objective correlates of nigral degeneration as well as investigating its temporal evolution. Moreover, it investigates whether beta bursts occur in healthy control animals. Due to lacking recordings of healthy subjects in human studies, this has not been shown before.

The aim of the present thesis was to investigate the relationship among dynamic beta burst properties, degeneration of the dopaminergic system over time and the pathophysiology of parkinsonian symptom generation. We presumed the following outcomes regarding burst characteristics:

- Beta bursts occur in all groups and share common features when compared to human data.
- The number of long beta bursts, time spent in bursts, burst amplitude and the overlap of STN and primary motor cortex (M1) bursts increase with time after 6-OHDA injection and is lowest in healthy control subjects (Tinkhauser et al., 2017a).
- Number of long bursts, time spent in bursts, burst amplitude and the overlap of STN and M1 bursts correlate positively with degeneration of dopaminergic neurons.

- We can classify successfully whether a subject is healthy or lesioned by including beta power and burst characteristics in the classification process.

In the following sections, we describe the experimental setup (Section 2.1), explain methods that we used to analyze beta bursts (Section 2), provide a summary of the results (Section 3) and finally discuss the implications of our results regarding clinical applications and future research (Section 4).

## 2 Material and Methods

### 2.1 Experiment

The present study capitalized on an ongoing effort to characterize oscillatory basal ganglia activity in relation to nigral degeneration in the Movement Disorders and Neuromodulation Unit. Electrode implants, recordings and histological examinations were conducted by Jens Haumesser and Christoph van Riesen, who provided the data for the present analysis. The experimental design included histological measurements from STR and the substantia nigra pars compacta (SNc), motor behavior and electrophysiological signals in the local field potential (LFP) from rats in different stages of the 6-OHDA lesion. In first analyses it was shown that beta power is correlated with behavioral and histological changes.

**Animals.** 46 male Wistar rats (Harlan Winkelmann, Germany) were used in accordance to the German Animal Welfare Act and European regulations. Animals had free access to water and food and were kept in standard housing conditions. Due to highly abnormal burst patterns, which we attributed to signal artifacts, we excluded one animal from STN burst analysis and one other animal from M1 burst analysis.

**Experimental Design.** Subjects were divided into one control group ( $n = 9$ ) and 4 experimental groups ( $n = 10$ ;  $n = 9$ ;  $n = 8$ ; and  $n = 10$ , respectively; Figure 1). Animals of the experimental groups were lesioned with the neurotoxin 6-OHDA. Animals of the control group were subjected to an injection of a solvent instead. In the four experimental groups, behavioral, electrophysiological and histological measurements were taken after a latency

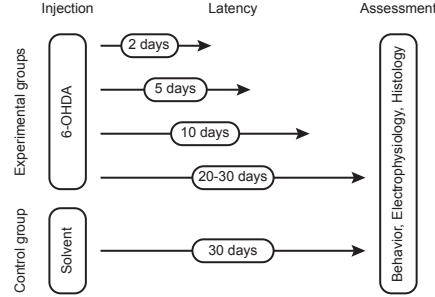


Figure 1: Experimental design. Animals received an injection of 6-OHDA or solvent on day 1. Depending on group, behavioral, electrophysiological, and histological data were recorded after 2, 5, 10 or 20–30 days.

of 2, 5, 10, and 20–30 days, respectively. All animals of the control group were measured after 30 days. Subsequently, behavioral and electrophysiological measurements were obtained. Directly after the recordings, animals were sacrificed to assess histological data of the nigrostriatal tract. Please note that due to the histological measurements, it was not possible to collect data in different lesion stages in the same animal—every animal underwent the experiment once only and was not included in more than one group.

**Lesion.** 1  $\mu$ l neurotoxin, dissolved in a solvent, or, in case of the control group, solvent only was injected. Animals received the injection unilaterally into the left medial forebrain bundle while being under urethane anesthesia. After the surgery, they were administered analgesic carprofen for three days to alleviate pain.

**Behavioral Measurements.** Two different tests to record characteristics of motor behavior were employed: the cylinder test (Schallert et al., 2000) and the drag test (Khaing et al., 2013), which both assess limb use asymmetry.

For the cylinder test, rats were placed in a transparent glass cylinder (height: 45 cm, diameter: 20 cm). While animals were vertically exploring the cylinder with the forelimbs, contacts of the left vs. right forelimb with

the cylinder were counted. Each trial was stopped when at least one forepaw had reached at least 15 contacts. It has been shown that 6-OHDA-lesioned animals exert a greater asymmetry than healthy animals by avoiding to use the impaired forelimb. Cylinder test scores show a very high correlation to dopamine depletion ( $r = 0.91; p < 0.001$ ) and a very high inter-rater reliability ( $r > 0.95$ ) (Schallert et al., 2000).

For the drag test, the rats' hind limbs were elevated while the forelimbs rested on the surface. Then the rat was dragged backwards and adjusting forepaw steps were counted for each side separately. One trial was ended when at least one side count reached 15 contacts with the ground.

We report results for both tests as relative ratios of the right (affected) to the left (unaffected) forelimb.

**Electrophysiological Recordings.** LFP in M1 was recorded by inserting two custom-made Ag/AgCl electrodes in the epidural space above the left M1. For STN recordings, a pair of microelectrodes was inserted above the left STN. Correct electrode placement was verified histologically post-mortem.

For referencing in M1 and STN recordings, two further electrodes were placed epidurally above the ipsi- and contralateral cerebellum, respectively. The raw 40 kHz-signal was bandpass-filtered (0.05 – 1000 Hz), amplified ( $\times 1750$ ) and downsampled to 1 kHz. All electrophysiological measurements were recorded under urethane anesthesia.

**Histology.** After electrophysiological recordings, the animals were sacrificed. Thereafter coronal brain sections of 40  $\mu m$  were prepared and sections from the STR and SNc for further analysis with tyrosine hydroxylase (TH) immunohistochemistry were selected.

For the SNc score, the number of TH-positive cells of the left (lesioned) SNc with the number of the right (intact) SNc was compared. The STR score was obtained by comparing the fiber density of the left dorsolateral STR to the density of the right dorsolateral STR.

Both scores represent the ratio of the left (lesioned) to the right (intact) side.

## 2.2 Data Analysis

**Preprocessing.** LFP recordings of one STN electrode and one M1 electrode per animal were selected manually according to the clearest signal without major artifacts.

Since electrophysiological recordings were obtained under urethane anesthesia, two cortical states emerged in the signal: slow wave activity and the activated state (Clement et al., 2008; Beck et al., 2016). The slow wave activity is dominated by slow frequency–high amplitude oscillations and resembles non-rapid eye movement sleep. In contrast, in the activated state, high frequency–low amplitude waves are more prominent. This state is comparable to the pattern that can be found in awake attentive animals. Since disease-related beta oscillations can be seen in the activated state only, all analyses were confined to this state: for every recording, one 50 seconds-episode of the signal was selected that showed a robust activated state pattern and was free of major artifacts.

It has to be noted that the all processing steps described above were conducted by members of the *Movement Disorders and Neuromodulation* group of the Charité Berlin and have been available when we started with the analyses described below.

**Time–frequency Analysis and Normalization.** We employed Morlet transformation to retrieve the *time–frequency representation* (TFR). We retrieve the TFR for every frequency  $f$  of the signal  $x(t)$  at time  $t$  with the convolution operation  $\otimes$ :

$$\text{TFR}(t, f) = x(t) \otimes w(t, f). \quad (1)$$

We write  $w(t, f)$  for the Morlet wavelet:

$$w(t, f) = Ae^{-t^2/2\sigma_t^2}e^{i2\pi ft}, \quad (2)$$

where  $\sigma_t$  is the *standard deviation* (SD) of the signal in the time domain and  $A$  is a normalization factor. In both time and frequency domain, Morlet wavelets are Gaussian shaped. Here,  $\sigma_f$  is the SD in the frequency at frequency  $f$ , given by  $\sigma_f = q/f$  and  $q$  is the width of the wavelet. The SD in time domain is given by  $\sigma_t = 1/(2\pi\sigma_f)$ . In this study, we used a frequency width of 10 cycles and a temporal width of  $3\sigma_t$ . We computed the wavelet transformation in steps of 5 ms at frequencies between 1 and 100 Hz, at a resolution of 1 Hz.

We normalized spectral density values by the cumulative average of the 8 to 12 and 31 to 90 Hz power.

**Definition of Beta Bursts and Related Parameters.** Since there is no standard procedure to define bursts in the rat model, burst analysis was adapted from Tinkhauser and colleagues (Tinkhauser et al., 2017a; Tinkhauser et al., 2017b).

For every subject and time bin, we averaged the signal across frequencies from 13 to 30 Hz and smoothed it in time employing *moving average* (200 ms). Figure 2 illustrates the definition of bursts schematically: the signal was labeled as *burst* when exceeding a given amplitude threshold (green line) for more than 100 ms. The blue array indicates the burst duration, which is defined as the time from the point when the amplitude exceeds the threshold to the point when the amplitude undergoes the threshold again. The amplitude is defined as the peak amplitude of the burst (red array). As the precise amplitudes of percentile-defined thresholds could vary between groups, we defined the threshold for STN and M1 separately as the 75th percentile of the amplitude distribution of all subjects and groups together. Thus, we applied the same threshold in every group, but used a different threshold for STN and M1 LFP recordings.

A burst was labeled to have a *long* duration when exceeding a cutoff of 350 ms; bursts shorter than the cutoff were labeled as *short*. We retrieved the parameter % *long bursts* by dividing the number of long bursts by the overall number of bursts per recording. The cutoff of 350 ms was chosen arbitrarily by visually inspecting burst durations. We discuss limitations of this procedure in Section 4. We derived the parameter *time spent in bursts* as the number of time bins during a burst divided by all time bins of the recording.

The *overlap* between STN and M1 bursts was calculated by deriving the fraction of time points during a burst in both STN and M1. We set a minimum overlap duration of 200 ms (procedure adapted from (Tinkhauser et al., 2017b)).

To avoid distortion of signal noise, all bursts that lasted longer than the median duration across subjects of all groups plus three standard deviations were detected as outliers and rejected from further analysis. The same procedure of outlier rejection was applied to time spent in bursts, amplitude and overlap.

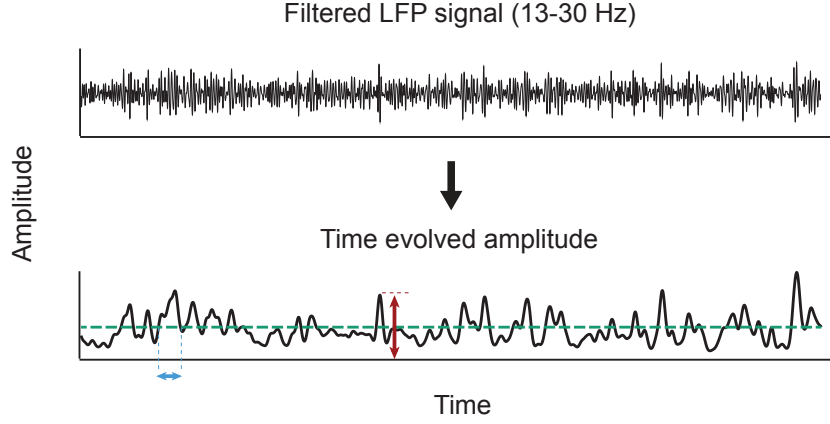


Figure 2: Definition of bursts. An example of a beta-filtered LFP signal (top) and the time evolving wavelet amplitude derived from the wavelet transformed signal (bottom). The green dashed line illustrates the threshold which defines onset and offset of the bursts. The blue array indicates the duration of a burst, the red array the amplitude. Adapted from Tinkhauser et al. (Tinkhauser et al., 2017b).

**Statistical Analysis.** We used non-parametric permutation testing to test whether the average of a parameter in the experimental groups differed significantly from the average in the control group, and to test whether the mean of a parameter was correlated with the group label (*control* = 1; *day 02* = 2; *day 05* = 3; *day 10* = 4 and *day 20 – 30* = 5). To test the correlation between burst characteristics and histology, we employed Spearman’s rank correlation. Additionally, we performed partial Spearman’s correlation analysis to determine to what extent correlations between burst parameters in STN and histological findings can be explained by changes in the respective burst parameter in M1 and vice versa.

We investigated whether a linear model of combinations of parameters as predictors would achieve a good prediction of STR and SNc scores. Thus, we calculated a linear stepwise regression, by using the Matlab function *stepwiselm*. We included all described parameters ( $x_1$  = beta power,  $x_2$  = % long bursts,  $x_3$  = time spent in bursts,  $x_4$  = burst amplitude and  $x_5$  = burst overlap) as independent variables and STR or SNc scores as dependent variables. Due to high correlation among all predictors we confined the model to a linear prediction without interaction of the predictors. Criterion for adding



or removing a term was the change in the value of the Akaike information criterion by adding or removing the term.

For classification we used Linear Discriminant Analysis (LDA). LDA is a common technique for pattern classification. Thus, it calculates the separability between different classes. We define three different dependent variables with two class labels each:

- Low vs. high STR score
- Low vs. high SNc score
- Experimental vs. control group.

We define the cutoff between low and high STR and SNc score at 100 %.

We used an *alpha* level of .05 for all statistical tests (\*  $p < .05$ ; \*\*  $p < .01$ ; \*\*\*  $p < .001$ ; \*\*\*\*  $p < .0001$ ). In both the tests of group differences and the correlation tests, four tests per parameter were conducted (group differences: day 02, day 05, day 10 and day 20–30 against control, respectively; correlation tests: STN–STR, STN–SNc, M1–STR, M1–SNc). To account for multiple comparison testing, we indicate when a p-value is not significant after bonferroni correction ( $\alpha_{\text{bonferroni}} = \alpha / 4 = .0125$ ). Group data are expressed as the mean  $\pm$  standard error of the mean.

We performed all analyses in MATLAB (MathWorks Inc.; R2017b) using *FieldTrip* and *Statistical Parametric Mapping open source toolboxes* (<http://www.ru.nl/fcdonders/fieldtrip>; <https://www.fil.ion.ucl.ac.uk/spm>) and with additional custom software.

## 3 Results

In the following section, we will summarize first results on behavior, histology and beta power. Afterwards we will present the results of the beta burst analysis.

### 3.1 Behavior

We express motor ability as use of the right (affected) forelimb relative to the left (unaffected) forelimb in %. Thus, a lower score indicates higher motor impairment.

Results from the cylinder test show a severe forelimb asymmetry already at day two after the lesion, in comparison to the control group ( $p < .0001$ ; Figure 3A). All other groups also show a significant reduction of test score (all  $p < .0001$ ). Drag testing reveals similar results (Figure 3A): relative to the control group, animals used their right forelimb much less at day two already ( $p < .0001$ ). Afterwards, the score remains relatively stable (see Table S1) and significantly different from the control group (all  $p < .0001$ ). The behavioral results show that the 6-OHDA injection lesioned the animals successfully. However, since we observe a clear bottom effect in behavioral test scores from day two, we will focus on histology data for further analysis.

### 3.2 Histology

Histological findings are expressed as STR fiber density or SNc cell count in the lesioned side compared to the intact side in %. Hence, lower scores indicate a higher loss of TH-positive fibers and neurons.

In both STR and SNc we observe a progressive degeneration of dopaminergic neurons over time (Figure 3B). Nigrostriatal fiber densities of all experimental groups are lower than in the control group (see Table S1, all  $p < .0001$ ). At the two latest time points, we find an almost total loss of fibers in STR.

Likewise, in SNc, averages of all time points differ significantly from the control group (day 02:  $p = .006$ ; day 05:  $p < .0002$ ; day 10:  $p < .0001$ ; day 20–30:  $p < .0001$ ; see Figure 3B and Table S1).

### 3.3 Beta Power

Figure 3C shows normalized power spectra from 5 to 40 Hz. The beta range from 13 to 30 Hz is shaded in gray. Whereas the spectra of the control group show only a slight deviance from the  $1/f$  distribution, the experimental groups demonstrate a clear peak in the beta range. The peak is visible in group day 10 already and is most pronounced in group day 20–30. The beta peak in the STN-day 20–30 signal is higher and more slim than in M1.

We obtain the mean power per group by averaging the power from 13 to 30 Hz and depict in Figure 3D. In STN the average power of day 10 and day 20–30 differ significantly from the control group (day 10:  $p = .007$ ; day 20–30:  $p = .0002$ ). Cortical data shows a significant increase of power at day 20–30 only ( $p = .004$ ), compared to the control group. However, we

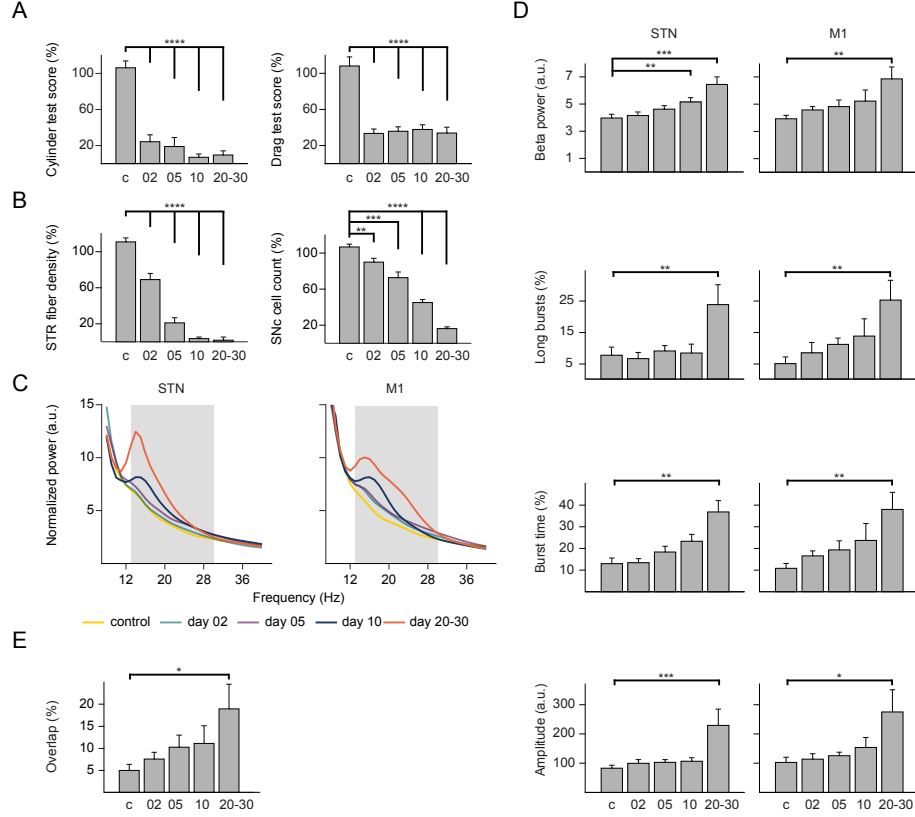


Figure 3: Average test data per group. (A) Group averages of the cylinder test (left) and the drag test (right). (B) Group averages of the relative fiber density in STR (left) and the relative number of TH-positive cells in the SNc (right). (C) Normalized power per group from 5 to 40 Hz in the STN (left) and M1 (right). The gray shaded area marks the critical beta range from 13 to 30 Hz. Power is elevated in the beta range in groups day 10 and day 20–30. (D) Group averages of beta power, relative number of long bursts, time spent in bursts and burst amplitude (top to bottom) in STN (left) and M1 (right). (E) Group averages of the relative overlap between STN and M1 bursts. Error bars represent the standard error of the mean. \*  $p < .05$  (not significant after bonferroni correction); \*\*  $p < .01$ ; \*\*\*  $p < .001$ ; \*\*\*\*  $p < .0001$ . c = control group, 02 = group day 02, 05 = group day 05, 10 = group day 10, 20–30 = group day 20–30.

observe a linear increase of beta activity over time points in both STN and M1 (correlation of mean power with group label STN:  $\rho = 1; p = .008$ ; M1:  $\rho = 1; p = .009$ ). The correlation between STN beta power and histology is highly significant for both STR and SNc scores (see Table 1 and Figure S1). However, the correlation between M1 beta power and histology is not significant after bonferroni correction (see Table 1).

### 3.4 Burst Duration

In Figure 4, we depict the burst length distribution for each group, binned into 6 categories: 100 to 225 ms, 225 to 350 ms, 350 to 475 ms, 475 to 600 ms, 600 to 725 ms and 725 to 850 ms. In general, shorter bursts occur more often than longer bursts. In both STN and M1, very short bursts appear to be more frequent in healthy animals and animals of group day 02. In contrast, subjects in group day 10 have fewer very short bursts and animals of group day 20–30 the least. Correspondingly, groups of higher latency after neurotoxin injection exhibit relatively more longer bursts. That is, with increasing duration the pattern shifts to relatively less bursts in the control group and more bursts for late latency groups.

When selecting only bursts of *long* ( $> 350$  ms) duration, we observe an increasing number of long bursts with time after injection (see Figure 3D and Table S1). However, in STN, the number of long bursts is only significantly higher in group day 20–30, compared to the control group ( $p = .006$ ). Likewise, also in M1, only the number of long bursts in group day 20–30 is significantly different from the control group ( $p = .009$ ). However, in M1 mean number of long bursts correlate significantly with the group label ( $\rho = 1; p = .009$ ). The percentage of long bursts in STN and M1 correlate negatively with both histology scores (Table 1, Figure S2). However, the correlation of STN and histology is not significant after bonferroni correction.

### 3.5 Time spent in bursts

Time spent in bursts in % indicates how much of the 50 sec recording time was part of a burst episode. In both STN and M1, the data show an increase of time spent in bursts with increasing measurement latency (see Figure 3D and Table S1). However, in both STN and M1 this change differs only in group day 20–30 significantly from the control group (STN:  $p = .003$ , M1:  $p = .002$ ). Mean time spent in bursts correlate significantly with the

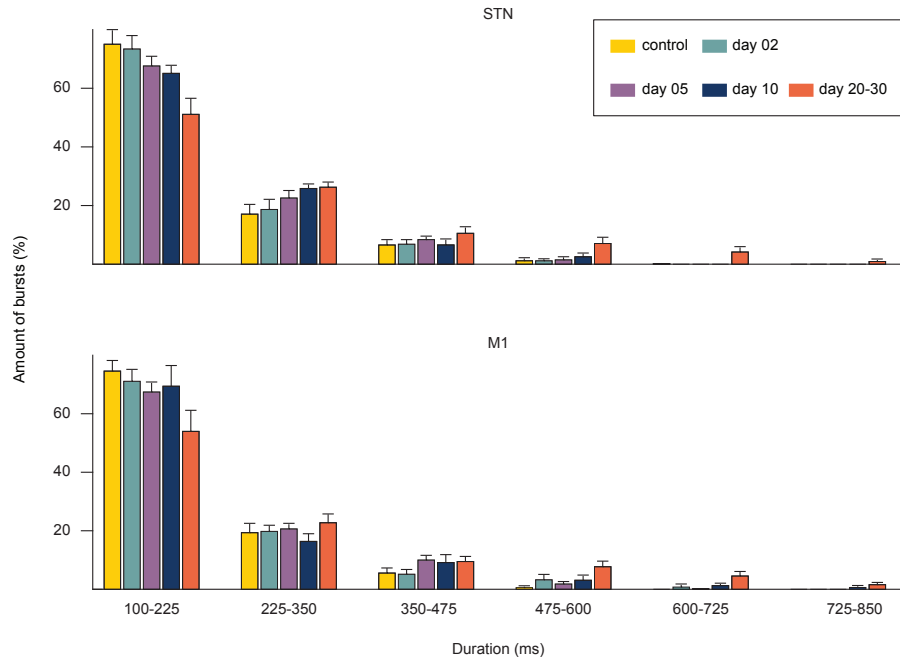


Figure 4: Burst durations per group. Shift in burst duration distribution in STN (top) and M1 (bottom). In more healthy groups the percentage amount of shorter bursts (100–225 ms) is higher, compared to highly impaired groups. With increasing burst duration the pattern shifts to relatively more bursts in impaired groups. Error bars represent the standard error of the mean.

Parameter	Structure	STR	STR (partial)	STR (w/o c.)	SNC	SNC (partial)	SNC (w/o c.)
fiber density	STR	–	–	–	.83 $p < .0001$	–	–
power	STN	–.50 $p = .0001$	–.42 $p = .005$	–.41 $p = .007$	–.58 $p < .0001$	–.51 $p = .0004$	–.51 $p = .0015$
power	M1	–.31 $p = .019^\dagger$	.05 n.s.	–.16 n.s.	–.33 $p = .014^\dagger$	.1 n.s.	–.17. n.s.
% long burst	STN	–.24 n.s.	.02 n.s.	–.27 n.s.	–.27 $p = .036^\dagger$	–.01 n.s.	–.23 n.s.
% long burst	M1	–.39 $p = .004$	–.31 $p = .04^\dagger$	–.31 $p = .03^\dagger$	–.39 $p = .004$	–.30 n.s.	–.26 n.s.
time spent in bursts	STN	–.50 $p = .0004$	–.42 $p = .0003$	–.44 $p = .004$	–.58 $p < .0001$	–.52 $p = .005$	–.54 $p = .0008$
time spent in bursts	M1	–.31 $p = .017^\dagger$	.06 n.s.	–.18 n.s.	–.33 $p = .016^\dagger$	.14 n.s.	–.17 n.s.
burst amplitude	STN	–.40 $p = .003$	–.23 n.s.	–.23 n.s.	–.46 $p = .0008$	–.39 $p = .009$	–.34 $p = .02^\dagger$
burst amplitude	M1	–.36 $p = .009$	–.12 n.s.	–.32 $p = .03^\dagger$	–.26 $p = .04^\dagger$	.08 n.s.	–.16 n.s.
overlap	STN-M1	–.31 $p = .02^\dagger$	–	–.23 n.s.	–.27 $p = .04^\dagger$	–	–.14 n.s.

Table 1: Spearman’s rank correlations between electrophysiological parameters and histology. For both STR and SNC, the correlation to both STN and M1 parameters are shown, as well as partial correlations and correlations where subjects from the control group were excluded (w/o c). Note that the partial correlation between an STN parameter and histology implicates that the influence of M1 was partialled out. Correspondingly, a partial correlation between a M1 parameter and histology implicates that the influence of STN was partialled out. <sup>†</sup> Correlation not significant after bonferroni correction.

group label in both STN and M1:  $\rho = 1, p = .007$  (STN);  $\rho = 1, p = .009$  (M1). Correlation between time spent in bursts in STN and histology is highly significant for both STR and SNc scores (see Table 1, Figure S3). Correlation between M1-time spent in bursts and histology is not significant after bonferroni correction (see Table 1).

### 3.6 Burst Amplitude

Besides the significant increase of beta burst amplitude in group day 20–30 in STN ( $p = .0006$ ) and M1 ( $p = .03$ ; not significant after bonferroni correction), we do not observe any other significant change of the amplitude (see Figure 3D and Table S1). Also for amplitude we find a significant correlation between mean and group label (STN:  $\rho = 1, p = .009$ ; M1:  $\rho = 1, p = .007$ ). Additionally, we observe a medium correlation between burst amplitude and histology measurements (see Table 1, Figure S4).

### 3.7 Overlapping Bursts

The mean percentage of overlapping bursts is significantly higher than zero in all groups (experimental groups:  $p < .0001$ , control group:  $p = .004$ ) and ranges from 5% in the control group to 19% in group day 20–30 (see Table S1). We observe a significant difference to mean overlap of the control group in group day 20–30 only ( $p = .018$ ; not significant after bonferroni correction; Figure 3E). However, the linear increase across time points after injection is visible in the correlation between mean overlap and group label ( $\rho = 1; p = .008$ ). Percent of overlapping bursts correlates significantly with both STR and SNc scores (see Table 1, Figure S5).

### 3.8 Correlation between Burst Duration and Amplitude

To replicate the results of Tinkhauser and colleagues (Tinkhauser et al., 2017b), we investigated the relationship between duration and amplitude. We correlate the burst duration of every occurring burst of every animal with the burst amplitude of the same burst. We observe a highly significant correlation between the two parameters (STN:  $\rho = .85; p < .0001$ ; M1:  $\rho = .88; p < .0001$ , see Figure S6). The correlation does not differ between groups (see Table S1).

### 3.9 Correlation without Control Group

Are correlations between the respective parameters and histology measures mainly driven by the difference between the control group and the experimental groups? To test whether a parameter does also vary with different degrees of the lesion, we computed all correlations without animals of the control group (see Table 1). While we find more stable correlations among the parameters in STN and histology in a majority of parameters, most correlations for M1 are eliminated. An exception is the correlation of long bursts with the STR score which stays stable for M1, but disappears for STN data.

### 3.10 Partial Correlations

To test whether the correlation between STN and histology are stable when controlling for the influence of M1, we conducted partial correlations. Results show that correlations remain stable in all parameters besides % long bursts (see Table 1). In contrast, when correlating parameters of M1 without the influence of the STN with histology, all effects besides the correlation between % long bursts and STR score are eliminated.

### 3.11 Low and High Beta

Literature has shown that differences between healthy and impaired subjects are generally more present in the low (13–20 Hz) than in the high (20–30 Hz) beta band (Priori et al., 2004). To investigate whether we can confirm this pattern in our data, we performed all analyses described above for low and high beta separately. We find slightly more prominent patterns for low beta, in comparison with high beta (data not shown). However, since differences were small and not significant, we concentrated all further analyses on the overall beta range from 13 to 30 Hz.

### 3.12 Stepwise Regression

In the sections above, we describe five different electrophysiological parameters, their variation across groups and their correlation with histology. To get clearer insight on the relative predictive value of these parameters in relation to histological data, we performed a stepwise multivariable linear regression. This way we aimed to find a model that fits STN or M1 electrophysiological



data to either of the dependent variables STR score ( $y_1$ ) or SNc score ( $y_2$ ). We included all parameters described above as independent variables: % long bursts ( $x_1$ ), beta power ( $x_2$ ), time spent in bursts ( $x_3$ ), burst amplitude ( $x_4$ ) and burst overlap ( $x_5$ ).

We conducted the regression separately for STN and M1 parameters. For STN data, we find that a combination of power and % long burst fits both histological data best. For both STR and SNc, we reach a high fit (STR:  $R^2 = 0.36$ ; SNc:  $R^2 = 0.47$ ; model formula and coefficients are summarized in Figure 5A). For M1 data, the % long bursts alone outperforms all other parameters and combinations by reaching a medium to high fit of  $R^2 = 0.18$  (STR) and  $R^2 = 0.19$  (SNc; see Figure 5B). In Figure S7 we show the estimated data of the respective models, performed with a leave-one-out validation. Since we observe many subjects whose % long burst score is at zero, we computed estimates and leave-one-out predictions without subjects with zero long bursts and depict them in Figure S8 and Figure S9. Without subjects with zero bursts, STN-% long bursts does not improve the model significantly and predicting with M1-% long bursts does not reach better estimates than a prediction with M1-power.

Finally, we ran a stepwise regression by including all parameters of STN and M1. Here we find that the combination of STN-power and STN-% long bursts outperform all other combinations (fits see above).

### 3.13 Classification

So far, we found quite robust correlations among electrophysiological parameters and histology. To investigate how well we can predict the stage of neuron degeneration with electrophysiology, we conducted an LDA with five-fold stratified cross-validation. We investigated classification accuracy for three different criteria (see Section 1): impaired (low) vs. intact (high) nigrostriatal fiber density; impaired (low) vs. intact (high) SNc cell count; and experimental groups vs. control group.

Including STN-power and STN-% long bursts, we reach an accuracy of 86.7 % for STR scores, 80.0 % for SNc scores and 82.2 % when taking groups as criteria. Combining M1-power and M1-% long bursts leads to a classification accuracy of 86.6 % for STR labels, 77.8 % for SNC labels, and 77.8 % for the group labels.

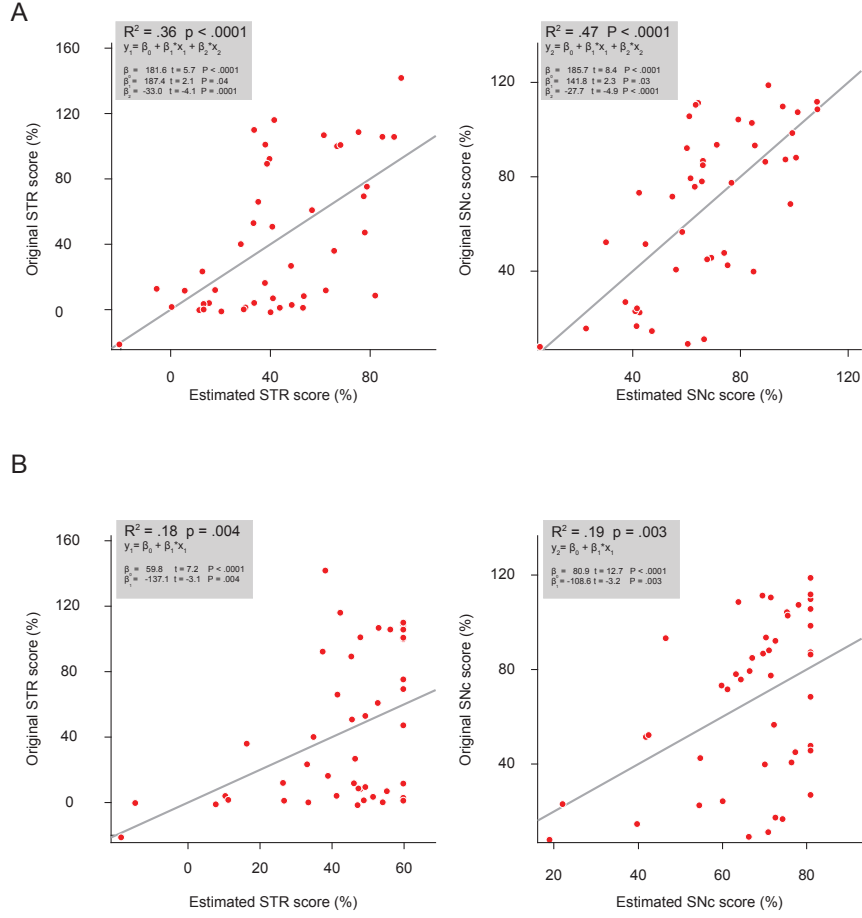


Figure 5: Original and estimated histology scores. (A) Histology data estimated from STN electrophysiology. Significant predictors are % long burst ( $x_1$ ) and beta power ( $x_2$ ) for both STR and SNc scores. (B) Histology data estimated from M1 electrophysiology. The model with only % long burst ( $x_1$ ) performs best for both STR and SNc scores.

## 4 Discussion

Three main conclusions may be drawn from this study: first, beta power and burst parameters—such as the proportion of long bursts or time spent in bursts—are highly correlated with the degree of nigrostriatal dopaminergic degeneration. Second, in a linear stepwise regression, a model with beta power and the percentage of long beta burst in the STN achieves the best fit to explain both STR and SNc variance. Third, we can distinguish healthy from lesioned subjects with a classification accuracy of over 80 %. These findings support the notion that beta parameters can serve as biomarkers for the stage of neuron degeneration.

In the present study, we find beta bursts in all groups, including the control group. This is an important finding, since beta bursts has not been studied in healthy subjects before. The finding suggests that beta bursts should not be mistaken as pathological per se. However, higher burst rates, a higher amount of long bursts and high-amplitude bursts seem to be more likely in PD (Tinkhauser et al., 2017a; Tinkhauser et al., 2017b).

**Motor Pathways.** In general, rhythmic oscillations in the brain are thought to build up a communication between neuronal ensembles (Fries, 2015). These rhythmic synchronizations propagate on specific networks and pathways. There are several pathways that build the *basal ganglia-motor cortex loop*, which is crucial for movement generation. The *indirect* pathway evolves from the cortex via the STR and the globus pallidum pars externa to the STN (Albin et al., 1995). From STN, the signal is forwarded via the globus pallidum pars interna to the thalamus. The SNc modulates signal processing in the indirect pathway with dopamine. Dopamine depletion results in inhibition of the thalamus (Albin et al., 1995). The *hyperdirect* pathway takes a shortcut from the motor cortex directly to the STN (West et al., 2018). A recent study of Neumann and colleagues (Neumann et al., 2018) shows that the indirect and the hyperdirect pathway play a different role in motor preparation and kinematics. There are several hypotheses on how the beta rhythm propagates in this circuit and why beta oscillations impact motor function in PD (Shin et al., 2017; Frank, 2006; West et al., 2018). However, the precise mechanism is still unclear. When we eliminated the influence of STN in the correlation between histology measurements and M1 parameters, the relation still remains stable in most parameters. In contrast, we do not find significant partial correlations between M1 and histology with-

out the influence of STN. Similarly, we find a more stable correlation among oscillatory STN-parameters and histology when leaving out the control group, compared to M1-parameters. It is not entirely clear why the relation association between beta characteristics and dopaminergic degeneration is more stable in the STN. While various factors may account for this observation, the direct loss of dopaminergic control over subthalamic afferents likely results in a more immediate disruption of local neuronal ensembles in the STN.

The occurrence of long beta bursts indicates that neurons are more likely to fire together. In this state, neurons do not carry information individually which leads to a limitation of the neuron’s coding capacity (Brittain and Brown, 2014). Normally, beta oscillations seem to play a functional role in motor slowing and decrease during movement initiation (Lofredi et al., 2018). However, long high-amplitude beta bursts, as observed in PD, might impair information coding on the network level (Feingold et al., 2015). This is, they appear to not be limited to local synchronizations but also involve pathological synchronization across several structures in the basal ganglia–cortical network (Tinkhauser et al., 2018). In the present study, we observed bursts that lasted up to 850 ms in both cortical and subcortical regions of the most affected animals. On average, we observed around 25 % long bursts in highly affected subjects. Also beta power was highly elevated. The severity of these alterations fits the notion that beta bursts build up by resonating in the long range motor loop, involving cortical ends of the loop as well as parts of the basal ganglia. In our analysis we show that the overlap between bursts in STN and M1 increases with the degree of neuron degeneration. For future work it would be interesting to take more stable and informative coherence measures to investigate the connectivity between both sites and to put it into context of neuron degeneration.

**Parkinson Therapy.** The cause of irregularities in motor cortex–basal ganglia circuit in PD is dopamine deficiency due to degeneration of dopaminergic neurons in the basal ganglia (Bernheimer et al., 1973). Thus, *levodopa*—a precursor of dopamine—is used for therapy of PD symptoms like akinesia (Postuma et al., 2015). Moreover, DBS of the basal ganglia at regular and high frequencies (in excess of 100 Hz) is an effective treatment of PD (Schuepbach et al., 2013; Deuschl et al., 2006). Kühn and colleagues (Kühn et al., 2008) showed that high frequency stimulation of the STN both suppresses beta activity and reduces motor impairments. While in conventional DBS

stimulation pulses occur at a constant frequency, *adaptive* DBS (or *closed-loop* DBS) monitors *biomarkers* and regulates pulses accordingly (Meidahl et al., 2017): adaptive DBS stimulates only while the marker exceeds a pre-set threshold. Closed-loop DBS appears to induce fewer side effects and is more effective than conventional DBS. In PD, the severity of an ongoing tremor has been shown to be a useful peripheral biomarker (Meidahl et al., 2017). However, a downside of peripheral markers is that they close the loop after the event (for example, an increase of tremor amplitude) already occurred. In contrast, *central* biomarkers make it possible to intervene earlier. Although it is not exhaustively clear whether beta power has a causal relation to PD symptoms (Sherman et al., 2016), it has been proposed as a biomarker for adaptive DBS in PD (Little et al., 2013). This gains further support from Neumann and colleagues (Neumann et al., 2017) who showed that the correlation between beta activity and motor symptoms in PD patients remain stable over the long term. The present study shows that it is possible to predict the state of dopaminergic degeneration in the substantia nigra with beta parameters with high accuracy. Beta parameters of the STN achieved slightly better predictions than parameters of M1. Class labels derived from STR scores could be predicted best. These findings support the idea to take beta power and beta burst properties as biomarkers for the pathophysiology of PD patients.

**Relation to Studies in Parkinson Patients.** Tinkhauser and colleagues (Tinkhauser et al., 2017a) compared PD patients who received either conventional DBS, adaptive DBS, or no stimulation. In conventional DBS, both short and long bursts were suppressed in proportion. In contrast, adaptive DBS increased the number of short beta bursts and decreased the number of long bursts. Thus, high-frequency stimulation seems to cut long beta bursts short, which has a positive effect on movement control. This finding is highly relevant, as the number of short bursts correlated negatively and number of long bursts positively with clinical impairment. In the study at hand, we had the unique opportunity to forge a link among cortical and subcortical beta parameters and the degree of dopaminergic neuron degeneration. We found a positive correlation between the relative number of long bursts and dopaminergic degeneration in the SNc. This supports the view of the pathological relevance of long beta bursts in PD patients.

In a further study (Tinkhauser et al., 2017b), the authors investigated the relation of beta burst characteristics with the dopaminergic state of PD patients. They found an increase of shorter, lower amplitude beta bursts when patients were treated with levodopa, in comparison to levodopa withdrawal. The present study did not compare ON- and OFF-medication PD patients but animals in different stages of a 6-OHDA lesion. However, both studies come to similar results. Especially the shift in the burst distribution from relatively-less short and relatively-more long bursts in highly impaired groups 4 compared to healthy controls, strongly resembles the pattern differences of OFF-medication patients, compared to ON-medication patients in (Tinkhauser et al., 2017b). To investigate the impact of levodopa on burst activity and histology, future studies could investigate beta burst characteristics in 6-OHDA-lesioned subjects that were treated with levodopa.

**Long Bursts and Histology.** To the best of our knowledge, the present study is the first investigation of the relation among beta bursts and histological data in a parkinsonian animal model. Our results suggest that beta power as well as the proportion of long burst in the LFP STN signal are well suited biomarkers for inferring the degree of neurodegeneration. When having only cortical electrophysiological signals on hand, the occurrence of long bursts may even be more informative than beta power. When considering the relatively-low correlation between STN-% long bursts and histology data, it seems surprising that this parameter outperforms other burst parameters in the stepwise regression. However, we found that STN-% long bursts has the lowest correlation to STN-beta power, in comparison to other parameters (data not shown). This indicates that % long bursts explains a variance share of the dependent variables that is not covered by prediction with beta power only. Additionally, we speculate that the distance of M1 to STN may act like a filter on long bursts: only in highly impaired animals, long bursts can also be seen in M1.

**Defining the Threshold.** Defining the 75th percentile threshold, which separates beta bursts from noise, has a large impact on amplitude and duration parameters. Choosing a low threshold includes more low-amplitude bursts than choosing a high threshold. In contrast, high-amplitude bursts are always included. Hence, the level of the threshold determines how many low-amplitude bursts are included in the analysis. This not only influences

amplitude parameters: since amplitude and duration are shown to be highly correlated, it also impacts duration parameters: bursts are truncated closer to their peak in case of a higher threshold, which leads to a shorter duration.

In our hypotheses (see Section 1) we expect that amplitude and duration vary across groups. Assuming that burst amplitude is lower in the control group than in the day 20–30 group, this poses a major confound when defining the threshold per subject: in the control group, more low-amplitude bursts lead to a lower threshold which in turn leads to including more low-amplitude bursts. Likewise, in the day 20–30 group, the occurrence of more high-amplitude bursts leads to a higher threshold, which leads to exclusion of the low-amplitude bursts that would have been in the signal. Hence, the difference between the two groups is more extreme than when taking the same threshold for both groups. Since the correlation between amplitude and duration does not change among groups (see Section 3.8), the same applies to duration parameters.

In the study of (Tinkhauser et al., 2017a), the authors implemented a within-subjects design and defined the threshold per subject, but applied the same threshold in all conditions. This procedure is reasonable to account for between-subjects variance in burst character that is not related to the experimental conditions. In the study at hand, this was not possible due to a between-subjects design. However, we assumed that unrelated burst variance would be randomly distributed among subjects of different groups. Thus, we decided to apply the same threshold—the average of all animals of all conditions—to all recordings.

**Limitations.** It has to be noted that the investigation of bursts is still new. In particular, there is no standard procedure for defining bursts yet. Thus, a number of decisions have to be made regarding normalizing, defining thresholds and determining the cut off between long and short bursts. In the sections above, we aimed to show our methodology as transparent as possible. However, we want to emphasize that parts of the analysis had an exploratory character and have to be replicated in the future.

Furthermore, it seems surprising that we observe a positive % long burst coefficient in the stepwise regression with STN parameters although the STN-% long bursts parameter correlates negatively with histology. Considering the results of the regression without subjects with zero long bursts, the percentage of long bursts may not be as predictive as seems at first sight. We suggest

to replicate our findings and further investigate the long burst–histology relationship before using them in clinical setups.

Besides, it could be that the animals were still recovering from the surgery in the day 02 group. This may have impaired their behavioral score and could explain the drastic drop of behavioral performance. This suggestion gains support from a finding of Deumens and colleagues (Deumens et al., 2002) who showed that about 50 % of dopaminergic cells in the SNc have already degenerated when PD symptoms start to emerge. To control for unspecific effects of surgery recovery, a control group at every time point after the surgery, especially after two days, would have been necessary.

## 5 Conclusion

Beta power and burst parameters are highly correlated with nigrostriatal cell loss. We can distinguish healthy from lesioned subjects with a high classification accuracy. This supports the idea that beta parameters can serve as biomarkers for the stage of neuron degeneration.



# Supplementary Material

Parameter	Structure	Control	day 02	day 05	day 10	day 20–30
cylinder test score (%)	n.a.	106.30 ± 7.20	24.27 ± 7.51	18.92 ± 9.91	7.02 ± 3.70	9.53 ± 4.24
drag test score (%)	n.a.	108.10 ± 10.06	33.46 ± 4.70	33.84 ± 4.83	37.83 ± 4.77	33.88 ± 6.05
fiber density (%)	STR	110.70 ± 4.18	68.91 ± 6.54	20.97 ± 5.32	3.49 ± 1.39	1.76 ± 3.08
cell count (%)	SNc	106.70 ± 3.10	89.90 ± 4.06	72.67 ± 6.02	45.14 ± 3.22	16.24 ± 1.82
Power (a.u.)	STN	3.97 ± .25	4.15 ± .23	4.62 ± .24	5.15 ± .29	6.37 ± .49
	M1	3.93 ± .25	4.58 ± .23	4.82 ± .46	5.22 ± .78	7.85 ± 1.28
long burst (%)	STN	7.61 ± 2.45	6.53 ± 1.82	8.97 ± 1.62	8.32 ± 2.74	23.76 ± 6.26
	M1	4.99 ± 2.03	8.48 ± 3.21	11.21 ± 1.95	13.89 ± 5.49	25.51 ± 6.25
time spent in bursts (s)	STN	12.96 ± 2.50	13.40 ± 2.00	18.34 ± 2.66	23.32 ± 3.06	36.85 ± 5.11
	M1	10.82 ± 2.15	15.57 ± 2.28	19.33 ± 4.07	23.69 ± 7.59	38.01 ± 7.77
burst amplitude (a.u.)	STN	108.48 ± 10.56	117.87 ± 13.18	131.61 ± 11.76	121.21 ± 13.02	269.65 ± 78.31
	M1	132.86 ± 20.61	139.23 ± 16.62	139.85 ± 15.6	161.82 ± 31.47	210.55 ± 36.82
overlap (%)	STN–M1	4.97 ± 1.38	7.56 ± 1.47	10.25 ± 2.68	11.11 ± 3.94	18.96 ± 5.60
dur–amp	STN	.82 ± .03	.79 ± .02	.86 ± .02	.82 ± .02	.88 ± .01
	M1	.84 ± .02	.81 ± .03	.85 ± .02	.87 ± .03	.87 ± .02

Table S1: Group averages and standard error of the mean for all parameters.

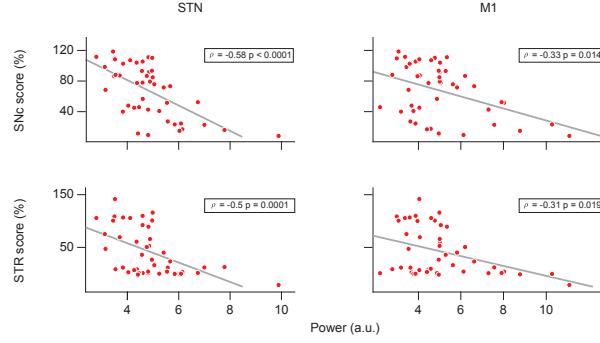


Figure S1: Power–histology correlation. Correlation between STN (left) and M1 (right) beta power and Snc cell count (top) and STR fiber density (bottom). Red dots represent single subjects. The gray lines indicate the first order fit between the two variables.

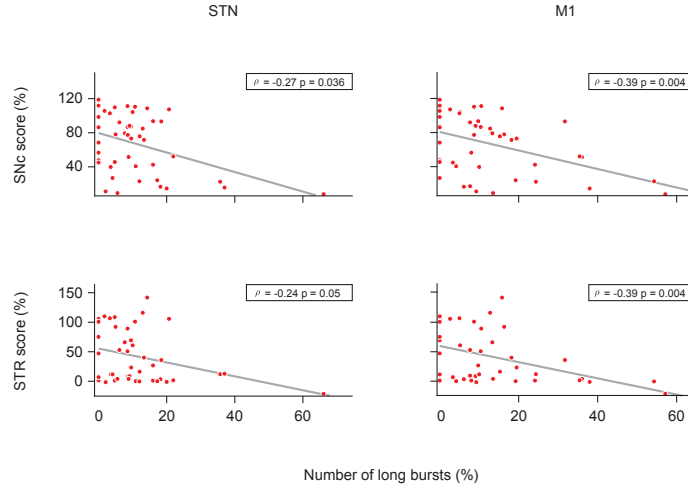


Figure S2: Correlation between proportional number of long bursts and histology. Red dots represent single subjects, gray lines indicate the first order fit between the two variables.

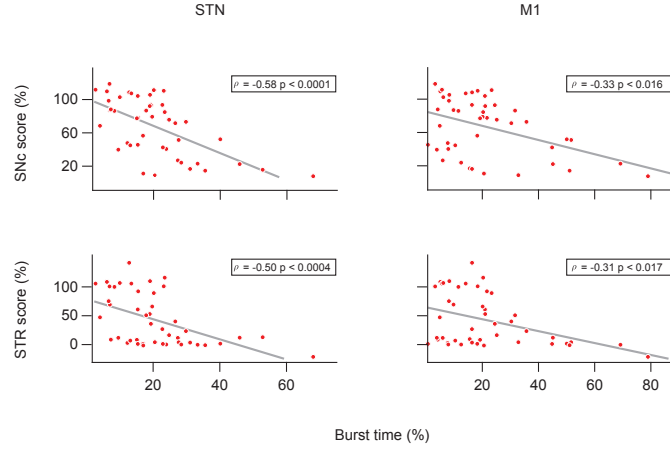


Figure S3: Correlation between time spent in bursts and histology. Red dots represent single subjects, gray lines indicate the first order fit between the two variables.

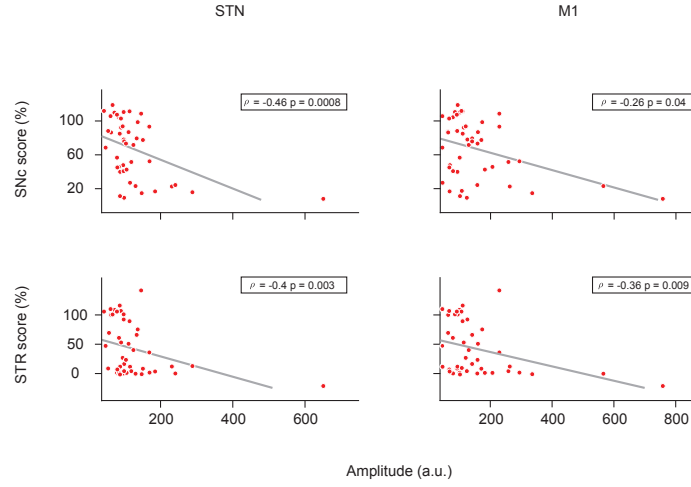


Figure S4: Amplitude-histology correlation. Red dots represent single subjects, gray lines indicate the first order fit between the two variables.

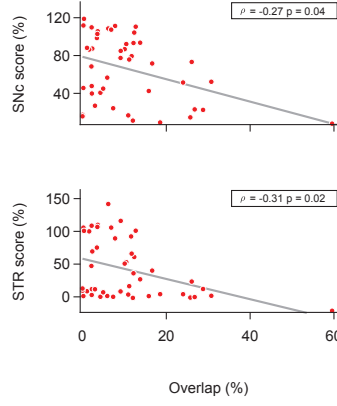


Figure S5: Correlation between the burst overlap and histology. Red dots represent single subjects, gray lines indicate the first order fit between the two variables.

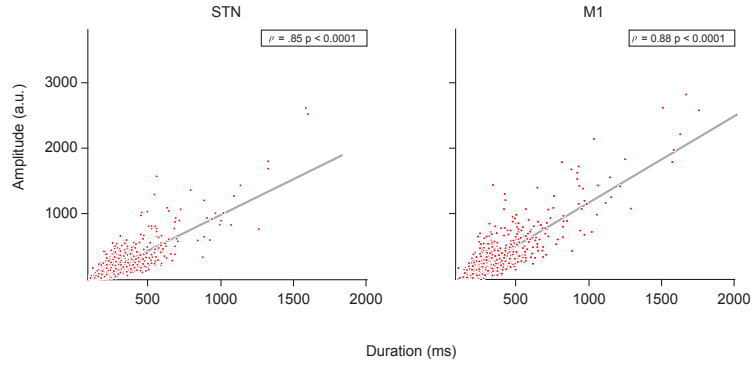
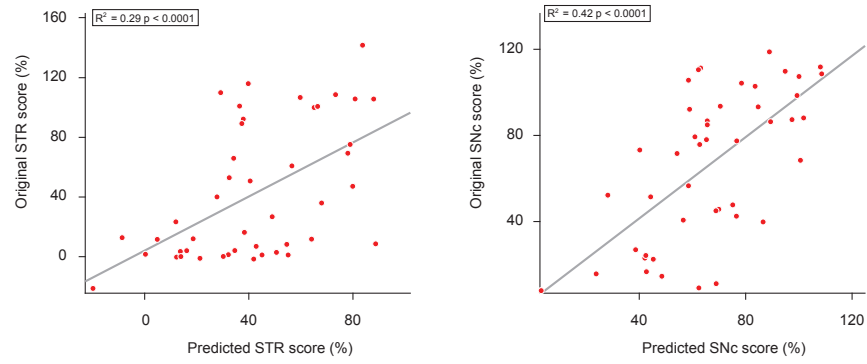


Figure S6: Correlation between burst duration and burst amplitude for all detected bursts across subjects and groups. Red dots represent single bursts, gray lines indicate the first order fit between the two variables.

A



B

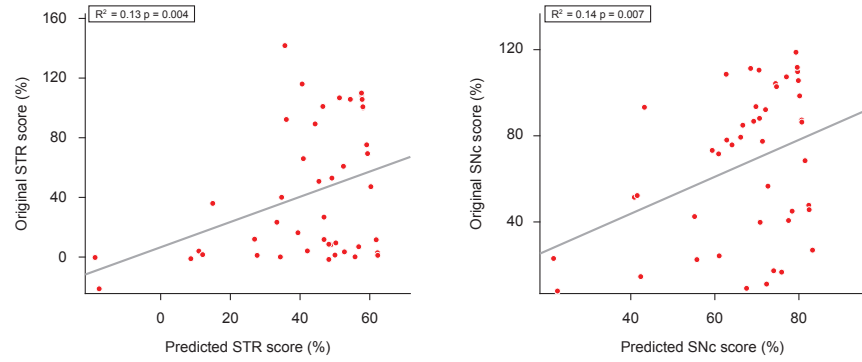


Figure S7: Original and predicted histology scores. (A) Prediction based on STN models. (B) Prediction based on M1 models. Cross-validated using a leave-one-out procedure.

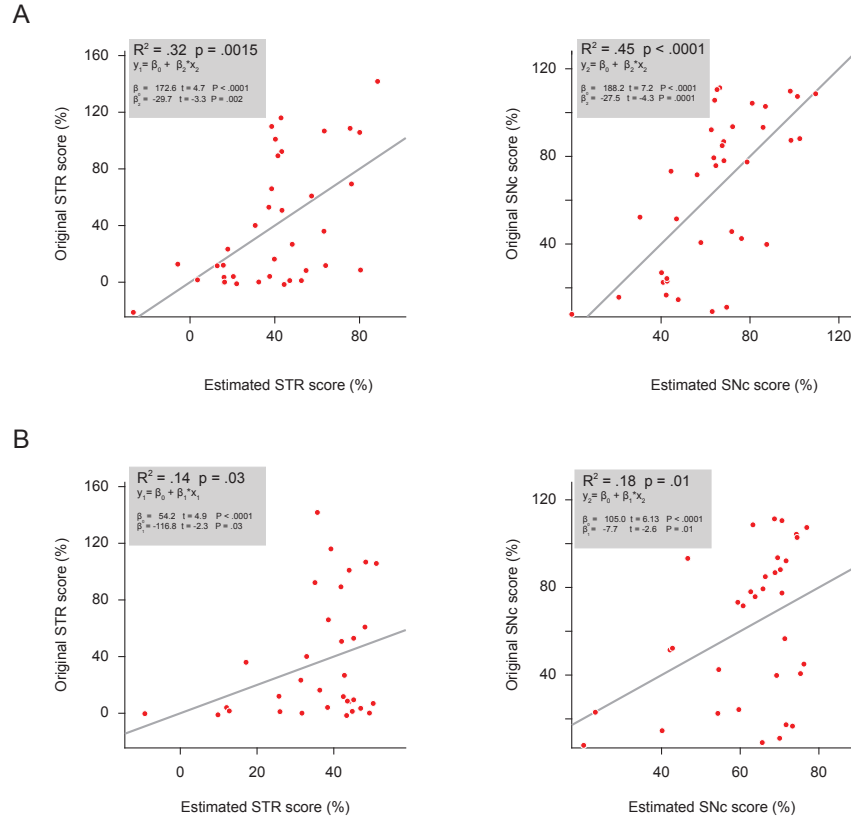


Figure S8: Original and estimated histology scores without subjects of zero long bursts. (A) STN-power ( $x_2$ ) as single predictor. (B) M1-% long ( $x_1$ ) bursts predicts the STR score best; M1-power ( $x_2$ ) predicts SNc scores.

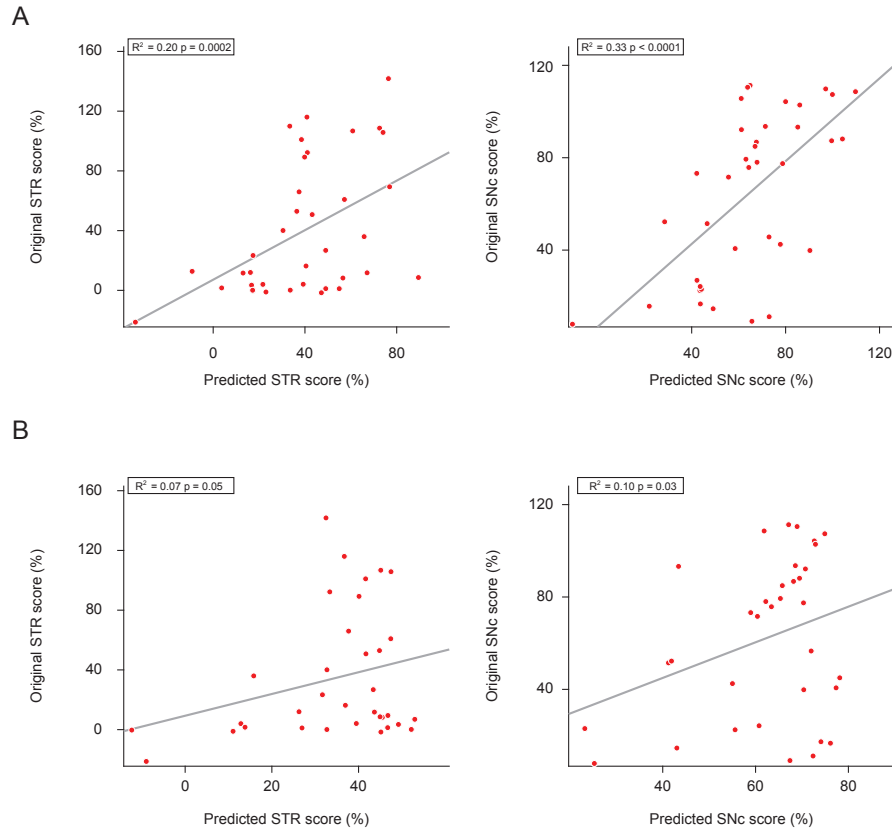


Figure S9: Original and predicted histology scores without subjects with zero long bursts. (A) Prediction based on STN models. (B) Prediction based on M1 models. Cross-validated using a leave-one-out procedure.

## References

- Albin, R., Young, A. B., and Penney, J. B. (1995). The functional anatomy of disorders of the basal ganglia. *Trends in Neurosciences*, 18(2):63–64.
- Beck, M. H., Haumesser, J. K., Kühn, J., Altschüler, J., Kühn, A. A., and van Riesen, C. (2016). Short- and long-term dopamine depletion causes enhanced beta oscillations in the cortico-basal ganglia loop of parkinsonian rats. *Experimental neurology*, 286:124–136.
- Bergman, H., Wichmann, T., and DeLong, M. (1990). Reversal of experimental parkinsonism by lesions of the subthalamic nucleus. *Science*, 249(4975):1436–1438.
- Bernheimer, H., Birkmayer, W., Hornykiewicz, O., Jellinger, K., and Seitelberger, F. (1973). Brain dopamine and the syndromes of parkinson and huntington clinical, morphological and neurochemical correlations. *Journal of the Neurological Sciences*, 20(4):415–455.
- Brittain, J.-S. and Brown, P. (2014). Oscillations and the basal ganglia: motor control and beyond. *NeuroImage*, 85 Pt 2:637–647.
- Clement, E. A., Richard, A., Thwaites, M., Ailon, J., Peters, S., and Dickson, C. T. (2008). Cyclic and sleep-like spontaneous alternations of brain state under urethane anaesthesia. *PloS one*, 3(4):e2004.
- Deumens, R., Blokland, A., and Prickaerts, J. (2002). Modeling parkinson’s disease in rats: an evaluation of 6-ohda lesions of the nigrostriatal pathway. *Experimental neurology*, 175(2):303–317.
- Deuschl, G., Schade-Brittinger, C., Krack, P., Volkmann, J., Schäfer, H., Bötzel, K., Daniels, C., Deutschländer, A., Dillmann, U., Eisner, W., and et al. (2006). A randomized trial of deep-brain stimulation for parkinsons disease. *New England Journal of Medicine*, 355(9):896–908.
- Feingold, J., Gibson, D. J., DePasquale, B., and Graybiel, A. M. (2015). Bursts of beta oscillation differentiate postperformance activity in the striatum and motor cortex of monkeys performing movement tasks. *Proceedings of the National Academy of Sciences of the United States of America*, 112(44):13687–13692.



- Frank, M. J. (2006). Hold your horses: a dynamic computational role for the subthalamic nucleus in decision making. *Neural networks : the official journal of the International Neural Network Society*, 19(8):1120–1136.
- Fries, P. (2015). Rhythms for cognition: Communication through coherence. *Neuron*, 88(1):220–235.
- Haber, S. N. (2003). The primate basal ganglia: parallel and integrative networks. *Journal of Chemical Neuroanatomy*, 26(4):317–330.
- Khaing, Z. Z., Geissler, S. A., Schallert, T., and Schmidt, C. E. (2013). Assessing forelimb function after unilateral cervical sci using novel tasks: limb step-alternation, postural instability and pasta handling. *Journal of visualized experiments : JoVE*, (79):e50955.
- Kühn, A. A., Kempf, F., Brücke, C., Gaynor Doyle, L., Martinez-Torres, I., Pogosyan, A., Trottenberg, T., Kupsch, A., Schneider, G.-H., Hariz, M. I., Vandenberghe, W., Nuttin, B., and Brown, P. (2008). High-frequency stimulation of the subthalamic nucleus suppresses oscillatory beta activity in patients with parkinson’s disease in parallel with improvement in motor performance. *The Journal of neuroscience : the official journal of the Society for Neuroscience*, 28(24):6165–6173.
- Kühn, A. A., Kupsch, A., Schneider, G.-H., and Brown, P. (2006). Reduction in subthalamic 8-35 hz oscillatory activity correlates with clinical improvement in parkinson’s disease. *The European journal of neuroscience*, 23(7):1956–1960.
- Little, S., Pogosyan, A., Neal, S., Zavala, B., Zrinzo, L., Hariz, M., Foltynie, T., Limousin, P., Ashkan, K., FitzGerald, J., Green, A. L., Aziz, T. Z., and Brown, P. (2013). Adaptive deep brain stimulation in advanced parkinson disease. *Annals of neurology*, 74(3):449–457.
- Lofredi, R., Neumann, W.-J., Bock, A., Horn, A., Huebl, J., Siebert, S., Schneider, G.-H., Krauss, J. K., and Kühn, A. A. (2018). Dopamine-dependent scaling of subthalamic gamma bursts with movement velocity in patients with parkinson’s disease. *eLife*, 7.
- Meidahl, A. C., Tinkhauser, G., Herz, D. M., Cagnan, H., Debarros, J., and Brown, P. (2017). Adaptive deep brain stimulation for movement dis-

- orders: The long road to clinical therapy. *Movement disorders : official journal of the Movement Disorder Society*, 32(6):810–819.
- Nambu, A., Tokuno, H., Hamada, I., Kita, H., Imanishi, M., Akazawa, T., Ikeuchi, Y., and Hasegawa, N. (1998). Excitatory cortical inputs to pallidal neurons via the subthalamic nucleus. *Neuroscience Research*, 31.
- Neumann, W.-J., Degen, K., Schneider, G.-H., Brücke, C., Huebl, J., Brown, P., and Kühn, A. A. (2016). Subthalamic synchronized oscillatory activity correlates with motor impairment in patients with parkinson’s disease. *Movement disorders : official journal of the Movement Disorder Society*, 31(11):1748–1751.
- Neumann, W.-J., Schroll, H., Marcelino, A. L. D. A., Horn, A., Ewert, S., Irmen, F., Krause, P., Schneider, G.-H., Hamker, F., and Kühn, A. A. (2018). Functional segregation of basal ganglia pathways in parkinson’s disease. *Brain*, 141(9):2655–2669.
- Neumann, W.-J., Staub-Bartelt, F., Horn, A., Schanda, J., Schneider, G.-H., Brown, P., and Kühn, A. A. (2017). Long term correlation of subthalamic beta band activity with motor impairment in patients with parkinson’s disease. *Clinical neurophysiology: official journal of the International Federation of Clinical Neurophysiology*, 128(11):2286–2291.
- Postuma, R. B., Berg, D., Stern, M., Poewe, W., Olanow, C. W., Oertel, W., Obeso, J., Marek, K., Litvan, I., Lang, A. E., Halliday, G., Goetz, C. G., Gasser, T., Dubois, B., Chan, P., Bloem, B. R., Adler, C. H., and Deuschl, G. (2015). Mds clinical diagnostic criteria for parkinson’s disease. *Movement disorders : official journal of the Movement Disorder Society*, 30(12):1591–1601.
- Pringsheim, T., Jette, N., Frolkis, A., and Steeves, T. D. L. (2014). The prevalence of parkinson’s disease: a systematic review and meta-analysis. *Movement disorders : official journal of the Movement Disorder Society*, 29(13):1583–1590.
- Priori, A., Foffani, G., Pesenti, A., Tamma, F., Bianchi, A. M., Pellegrini, M., Locatelli, M., Moxon, K. A., and Villani, R. M. (2004). Rhythm-specific

- pharmacological modulation of subthalamic activity in parkinson’s disease. *Experimental neurology*, 189(2):369–379.
- Schallert, T., Fleming, S. M., Leasure, J. L., Tillerson, J. L., and Bland, S. T. (2000). Cns plasticity and assessment of forelimb sensorimotor outcome in unilateral rat models of stroke, cortical ablation, parkinsonism and spinal cord injury. *Neuropharmacology*, 39(5):777–787.
- Schapira, A. H. V., Tolosa, E., Chaudhuri, K. R., and Poewe, W., editors (2015). *Non-motor symptoms of Parkinson’s disease*. Oxford University Press, Oxford, 2 edition.
- Schuepbach, W., Rau, J., Knudsen, K., Volkmann, J., Krack, P., Timmermann, L., Hälbig, T., Hessekamp, H., Navarro, S., Meier, N., and et al. (2013). Neurostimulation for parkinsons disease with early motor complications. *New England Journal of Medicine*, 368(7):610–622.
- Sharott, A., Magill, P. J., Harnack, D., Kupsch, A., Meissner, W., and Brown, P. (2005). Dopamine depletion increases the power and coherence of beta-oscillations in the cerebral cortex and subthalamic nucleus of the awake rat. *The European journal of neuroscience*, 21(5):1413–1422.
- Sherman, M. A., Lee, S., Law, R., Haegens, S., Thorn, C. A., Hämäläinen, M. S., Moore, C. I., and Jones, S. R. (2016). Neural mechanisms of transient neocortical beta rhythms: Converging evidence from humans, computational modeling, monkeys, and mice. *Proceedings of the National Academy of Sciences*, 113(33).
- Shin, H., Law, R., Tsutsui, S., Moore, C. I., and Jones, S. R. (2017). The rate of transient beta frequency events predicts behavior across tasks and species. *eLife*, 6.
- Tinkhauser, G., Pogosyan, A., Little, S., Beudel, M., Herz, D. M., Tan, H., and Brown, P. (2017a). The modulatory effect of adaptive deep brain stimulation on beta bursts in parkinson’s disease. *Brain : a journal of neurology*, 140(4):1053–1067.
- Tinkhauser, G., Pogosyan, A., Tan, H., Herz, D. M., Kühn, A. A., and Brown, P. (2017b). Beta burst dynamics in parkinson’s disease off and on

dopaminergic medication. *Brain : a journal of neurology*, 140(11):2968–2981.

Tinkhauser, G., Torrecillos, F., Duclos, Y., Tan, H., Pogosyan, A., Fischer, P., Carron, R., Welter, M.-L., Karachi, C., Vandenberghe, W., Nuttin, B., Witjas, T., Régis, J., Azulay, J.-P., Eusebio, A., and Brown, P. (2018). Beta burst coupling across the motor circuit in parkinson’s disease. *Neurobiology of disease*, 117:217–225.

West, T. O., Berthouze, L., Halliday, D. M., Litvak, V., Sharott, A., Magill, P. J., and Farmer, S. F. (2018). Propagation of beta/gamma rhythms in the cortico-basal ganglia circuits of the parkinsonian rat. *Journal of neurophysiology*, 119(5):1608–1628.